In Vitro Tobramycin Elution Analysis from a Novel β-Tricalcium Phosphate–Silicate-Xerogel Biodegradable Drug-Delivery System

Michael DiCicco,[1] Aaron Goldfinger,[1] Felix Guirand,[2], Aquill Abdullah,[2] Susan A. Jansen[1]

[1] Department of Chemistry: Analytical Chemistry, College of Science and Technology, Temple University, Beury Hall Rm. 201 13th and Norris Streets, Philadelphia, Pennsylvania 19122

[2] Department of Chemistry, Community College of Philadelphia, 1700 Spring Garden Street, Philadelphia, Pennsylvania 19130

Received 8 May 2003; revised 10 October 2003; accepted 21 October 2003
Published online 9 February 2004 in Wiley InterScience (www.interscience.wiley.com). DOI: 10.1002/jbm.b.30014

Abstract: This *in vitro* research analyzed local tobramycin elution characteristics from a novel, biodegradable drug delivery system, consisting of a β-TCP bone substitute, VITOSS™, encapsulated with silicate xerogel prepared by the sol-gel process. Tobramycin elution from silicate-xerogel-encapsulated VITOSS was compared directly with non-silicate-xerogel-encapsulated VITOSS to assess whether xerogels are effective in delivering greater tobramycin quantities in a controllable, sustained manner crucial for microbial inhibition. Tobramycin elution characteristics indicate an initial release maximum during the first 24 h that diminishes gradually several days after impregnation. The copious tobramycin quantity eluted from the VITOSS/silicate-xerogel systems is attributed to various factors: the intrinsic ultraporosity and hydrophilicity of VITOSS, the ability of tobramycin to completely dissolve in aqueous media, tobramycin complexation with highly polar SO_4^{2-} salts that further assist dissolution, and ionic exchanges between VITOSS and the environment. Silicate-xerogel–encapsulated VITOSS eluted 60.65 and 61.31% of impregnated tobramycin, whereas non-silicate-xerogel–encapsulated VITOSS eluted approximately one-third less impregnated tobramycin, at 21.53 and 23.60%. These results suggest that silicate xerogel optimizes tobramycin elution because of its apparent biodegradability. This mechanism occurs through xerogel superficial acidic sites undergoing exchanges with various ions present in the leaching buffer. Tobramycin elution kinetics were evaluated, and demonstrate that first-order elution rate constants are considerably less when silicate xerogels are employed, following a more uniform exponential decay-type mechanism, thus bolstering controlled release. Overall, tobramycin elution rates adhere to linear-type Higuchi release profiles. Elution rate constants are initially first order, and taper into zero-order elution kinetics in the latter stages of release. Because VITOSS and silicate xerogel are completely biodegradable, essentially all impregnated tobramycin will be delivered to the surgical site after implantation. © 2004 Wiley Periodicals, Inc. J Biomed Mater Res Part B: Appl Biomater 70B: 1–20, 2004

Keywords: β-tricalcium phosphate; silicate xerogel; tobramycin; drug-delivery system; fluorescence

INTRODUCTION

In the United States between 1996 and 2000, the cumulative retirement rate was 15.6% of the full-time permanent (FTP) workforce, or approximately 243,000 people. By the end of 2001, the United States Office of Personnel Management had projected that 3.4% of the FTP workforce would retire, equating to approximately 51,000 people. This number is expected to grow and reach 19%, or 281,000 people, in 2005. With the increasingly aging population, there is an increasing need for surgical treatment of degenerative musculoskeletal diseases.[1]

Chronic osteomyelitis, a common infectious bone disease, is characterized by bone necrosis and poor bone vascularization, and is accompanied by infection of the bone and surrounding tissues by bacteria. The type of bacteria isolated from osteomyelitis patients usually depends on the age of the patient and how the infection was acquired. Isolates from patients who acquire osteomyelitis from trauma or recent surgery are typically *Staphylococcus aureus.* Patients who suffer from chronic osteomyelitis generally are infected with *Staphylococcus epidermis*, *Pseudomonas aeruginosa*, *Serra-*

Correspondence to: Michael DiCicco, Department of Chemistry: Analytical Chemistry, College of Science and Technology, Temple University, Beury Hall Rm. 201, 13th and Norris Streets, Philadelphia, PA 19122 (e-mail: mikedicicco2001@yahoo.com)

tia marcescens, and *E. coli.* There are three classifications of osteomyelitis: acute hematogenous, subacute focal contiguous, and chronic osteomyelitis.[2] Chronic osteomyelitis, the most difficult case from a treatment perspective, involves the metaphyses of the bone (bone endings). The difficulty in treatment lies in the fact that because the metaphyses become infected, the joints, ligaments, and tendons serve as conduits for migration.[3]

Because of the poor vascularization of bone and surrounding regions, chronic osteomyelitis is primarily treated by surgical debridement of necrotic tissue followed by systemic administration of antibiotics and continuous irrigation of the lesion. Bone grafts are performed secondarily to treat any bone defects. These treatments, however, are associated with major invasion of pathogens, deep sepsis, other bacterial infections, and have effects on other organs during and after implant fixation.[4] Moreover, administering antibiotics through systemic routes would require high serum concentrations via large doses over short time intervals to achieve high local levels of the antibiotic to pervade the decaying tissue. Administration of high doses of antibiotics at the systemic level introduces the risk for systemic toxicity.[5–7] These toxic effects are especially pronounced in children and in the elderly. Therefore, to improve patient outcomes, it is necessary to provide a more effective drug-delivery method for local delivery of antibiotics. The focal application of antibiotics in surgical procedures offers an additional therapeutic approach to the treatment of infections and the possibility of minimizing systemic use of antibiotics.[8–11] Antibiotic-impregnated bone cements facilitate the localized delivery of the drug where it is most crucially required from the cement–bone interface to prevent infections. Over an extended time period, the antibiotic is released at high concentrations to the bone and/or tissue area to prevent or treat an existing infection while encouraging new bone formation. This highly localized delivery of the antibiotics is advantageous and more effective than traditional systemic routes where antibiotics are vulnerable to metabolization and devascularization of bone after a surgical procedure.

The initiative to encapsulate antibacterial agents for local administration has existed for over 30 years. In 1970, Buchholz and Engelbrecht introduced the idea of impregnating antibiotics into polymethylmethacrylate (PMMA) beads for bone cements.[12] By 1977, PMMA beads were being used notably to encapsulate gentamicin for arthroplastic bone cements and treatment of musculoskeletal infections. Today, PMMA-based polymerizable bone cements have found wide use in orthopedic prosthetic implant surgery. These cements are also used in several dental procedures. The incorporation of antibiotics into bone cements during the last two decades has become an accepted clinical practice and has had the advantage of preventing and treating orthopedic infections that result from implantation. Almost 90% of all orthopedic surgeons in the United States use antibiotic-impregnated bone cements as well as for temporary beads and spacers during revision surgery.[8]

Antibiotics in bone-void fillers must be able to elute in therapeutic concentrations and possess excellent aqueous solubility. They must also possess a wide spectrum of antimicrobial activity against a vast array of clinically relevant pathogens. Aminoglycosides are a diverse class of antibiotics that possess these attributes. They are essentially carbohydrates derived from microorganisms containing several aminoglycosidic linkages.[13] In fact, several aminoglycoside antibiotics have been shown to possess superior elution properties when impregnated in bone cements compared to other non-aminoglycosidic antibiotics such as the peptide-based vancomycin.[14–16] Aminoglycosides are categorized as concentration-dependent agents. That is, the rate of bacterial elimination increases with increasing aminoglycoside concentration. One of the most common aminoglycoside-type antibiotics, tobramycin, is the most widely used in orthopedic applications. Tobramycin has been shown to be effective against gram-positive and gram-negative aerobic organisms, and some mycobacteria. Tobramycin possesses superior activity *in vitro* and in clinical infections against *Staphylococcus aureus* (coagulase-positive and coagulase-negative); *Pseudomonas aeruginosa*; *Proteus sp* (indole-positive and indole-negative), including *P. mirabilis* and *P. vulgaris*; *E. coli*; *Citrobacter sp*; *Serratia marcescens*; and *Providencia sp*. However, tobramycin has been shown to have a low order of activity against *Streptococcus pneumoniae* and *enterococci*, and is completely inactive against any anaerobic bacteria.[17] Some studies even suggest that tobramycin is less nephrotoxic than other aminoglycoside antibiotics. Despite many years of investigation, it is not clear how tobramycin and other aminoglycoside antibiotics cause bacterial cell death. It is known that tobramycin binds irreversibly to one of two aminoglycoside receptor sites on the 30S ribosomal subunit, which, in turn, inhibits bacterial protein synthesis, caused by bacterial misreading of messenger-RNA.[18] Moreover, the degree of misreading messenger-RNA has been found to be a concentration-dependent phenomenon, and the drug may affect multiple ribosomal subunits.[13] Against gram-negative aerobic rods, tobramycin exhibits a post-antibiotic effect (PAE). PAE is where suppression of bacterial growth continues after the antibiotic concentrations fall below the minimum inhibitory concentration (MIC). The tobramycin MIC correlates are 2–4 parts per million (ppm) for susceptibility and 8–30 ppm for resistance *in vivo*. Tobramycin possesses five primary amine functionalities ($R\text{-}NH_2$). The chemical structure and chemical designation of tobramycin is illustrated in Figure 1. The melting/decomposition temperature for tobramycin (~287 °C) has also been reported, and is sufficiently high in preventing degradation when used in conjunction with bone cements having an exothermic polymerization.[19] This antibiotic can be loaded evenly and thoroughly into various bone cements typically by a simple hand-mixing procedure that surgeons employ. Tobramycin is adequately polar, which should indicate a good leaching potential from bone cements into an aqueous media.

Current drug-delivery systems fall into two categories: biodegradable and nonbiodegradable. Nonbiodegradable

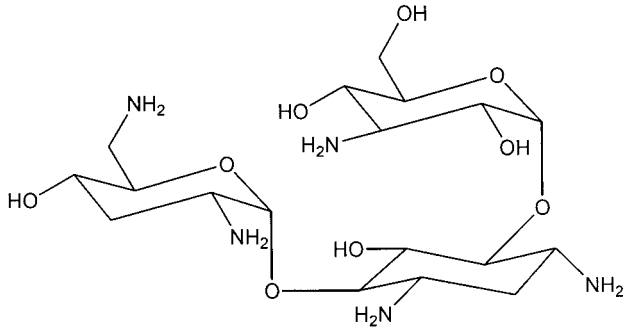

Figure 1. Chemical structure and designation of tobramycin.

drug delivery systems are typically PMMA bone cements or beads. Biodegradable forms of drug-delivery systems are more varied, and include the following: collagen sponges soaked with an antibiotic,[20,21] apatite-wollastonite glass ceramic,[22,23] hydroxyapatite,[24–27] β-tricalcium phosphate (β-TCP) [$Ca_3(PO_4)_2$],[28–31] polylactide/polyglycolide implants,[32] fibrin clots,[33] and polyurethanes.[34] Hydroxyapatite and β-TCP have been shown to be appreciably bioactive.[35] Silicate xerogels ($n SiO_2$) have also gained wide notoriety as a biodegradable drug vehicle as a result of their bioactivity and other attractive properties.[36–42] Furthermore, one study revealed that a biodegradable quinoline-polyacetate system had concentrations 100–1000 times above MIC for methicillin-resistant strains.[43] Finally, there are studies under way that are investigating the potential use of biodegradable fusidic acid in delivery systems.[44]

Each system has its advantages and disadvantages. Nonbiodegradable systems are limited by the types of antimicrobial agents they can deliver due to high exothermic polymerization leading to degradation of the active agent. They require a need for follow-up surgery to remove temporary PMMA devices, and certain bacteria strains produce a biofilm that adheres to the PMMA surface, perhaps providing a mechanism for recurrence of infection.[43] Biodegradable systems have an advantage over nonbiodegradable systems because of the fewer number of surgeries required for treatment. However, both nonbiodegradable, as well as some biodegradable systems need to be sterilized prior to implantation, especially apatite-reinforced polymers. Sterilization procedures usually entail ethylene oxide or gamma (γ) irradiation, with the latter known to facilitate degradation as well as promote cross linking of the polymer network.[45] Biodegradable systems are also limited by the rate of capsule degradation. Nevertheless, there are several criteria that must be addressed when choosing a material for a drug delivery system. First, the material must be biocompatible, not rejected by the body, and not cause adverse effects. Furthermore, a suitable implant will be bioactive, enhancing the formation of hydroxyapatite (bone growth). Second, the material must have mechanical strengths comparable to natural bone, which it is replacing. Third, the material and its degradation products should not enter systemic circulation, where it can exhibit various fates throughout the body.

The aim of this *in vitro* dynamic analysis is to quantitatively characterize the local elution of tobramycin as a function of time from a novel, biodegradable drug-delivery system, consisting of a β-TCP bone substitute, VITOSS™, encapsulated with silicate xerogel prepared by the sol-gel process. This was performed in order to test the ability of the silicate xerogel to control the release of tobramycin. VITOSS has been marketed in the United States, Europe, and Australia for the past several years. Sol-gel–fabricated silicate xerogel was chosen because it provides a means to prepare homogeneous high-purity materials with tailored chemical and physical properties[46] without using templating agents, its pore size can easily be controlled for various requirements, and silicon dioxide is relatively inert to the body.

EXPERIMENTAL DESIGN

Materials and Materials Description

VITOSS was purchased from Orthovita® (Malvern, PA). Tobramycin was obtained from Professional Compounding Centers of America, Inc. (Houston, TX). CBQCA© fluorescent dye kits were ordered from Molecular Probes (Eugene, OR). Phosphate-buffered saline (PBS) and hydrochloric acid (HCl) were purchased from Fischer Scientific (Pittsburgh, PA). Tetraethyl orthosilicate (TEOS) and tetrahydrofuran (THF) were purchased from Sigma-Aldrich Co. (Milwaukee, WI). All assays were analyzed with the use of a standard spectrofluorometer (FP-750, Jasco, Japan). All test materials and reagents were prepared according to the instructions provided by the manufacturers.

Calcium-phosphate-based cements are synthetic scaffolds that have been used in dentistry since the early 1970s and in orthopedics since the 1980s,[35] and have demonstrated a good safety record as synthetic bone void fillers.[47] Because TCP dissolves relatively rapidly, it readily undergoes remodeling and osteoclastic resorption, which in turn stimulates osteoblastic activity to regenerate bone. TCP ceramics have a stoichiometry similar to amorphous biological precursors to bone. Although calcium-phosphate-based products have been studied for bone repair for 80 years, principally the so-called high-temperature calcium phosphate, such as β-TCP and hydroxyapatite, or some combination of the two, have predominated in recent medical studies.[48] VITOSS is an ultraporous scaffold processed from β-TCP particles averaging 100 nanometers (nm) in size, mimicking the structure of natural cancellous bone, thereby rendering it as an appropriate substitute as an alternative to autografts and allografts in trauma and spinal arthrodesis surgery.[49] Its interconnected microporosity, which more closely resembles the trabecular structure of human cancellous bone, distinguishes VITOSS from earlier calcium-based ceramics. This extensive ultraporosity, which is effortlessly convened in the scanning electron microscopy (SEM) micrograph contained in Figure 2, appears to facilitate more rapid vascular invasion and fluid communication. This novel material has a broad range of pore sizes (1

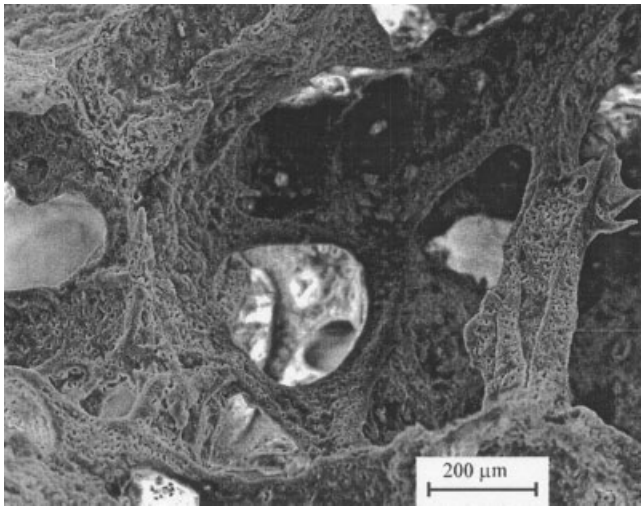

Figure 2. SEM micrograph of ultraporous VITOSS portraying its inherent interconnected porosity and microporosity.

μm–1 mm); possesses higher porosity (90% by volume) than conventional TCPs, exposing a larger surface area to cells and nutrients; and is more readily soluble than synthetic hydroxyapatite. Additional surface area facilitates faster and more complete bioresorption. Nanometer-sized particles (average diameter 100 nm) aid in this regard; smaller fragments within the scaffold are shown to convey greater surface-area osteoconductivity and to facilitate osteoclastic digestion during remodeling. On the other hand, the larger pores facilitate new bone ingrowth and vascularization; smaller pores and inherent hydrophilicity improve capillarity to wick nutrients, blood, cellular elements, marrow, and growth factors. A visual demonstration of the wicking capability of VITOSS is exhibited in Figure 3. The three-dimensional, multidirectional scaffolding is supplied as block pieces that may be shaped at the time of surgery and tamped into position, or as morsels for packing into irregularly shaped bone voids (refer to Figure 4). A complete summary of the various properties of VITOSS compared to hydroxyapatite is reported in Table I.

The sol-gel process alludes to the series of hydrolysis and condensation reactions involving alkoxy silanes such as TEOS or tetramethyl orthosilicate (TMOS) and alkoxy titanates[50] whereby addition of an acid catalyst yields a gelatin-like polymer. The term *sol-gel* is derived from the fact that the reaction begins as a solution and quickly polymerizes to form a gelatin. The sol-gel process is a very well studied set of reactions[46,51–55] dating back to1955, when Roy and Roy[56] prepared an array of composites from TEOS and metal nitrate salts. The acidity of the reaction media, the content of water, and the solvents are known to play a critical role in the sol-gel reaction. The reaction of TEOS in conjunction with an acid catalyst proceeds in four stages and is reversible up to 673 K:

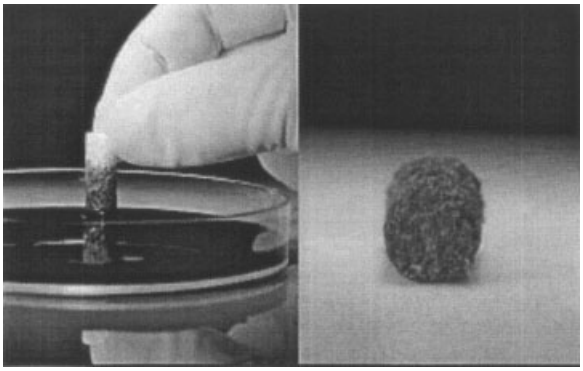

Figure 3. Demonstration of VITOSS block wicking blood.

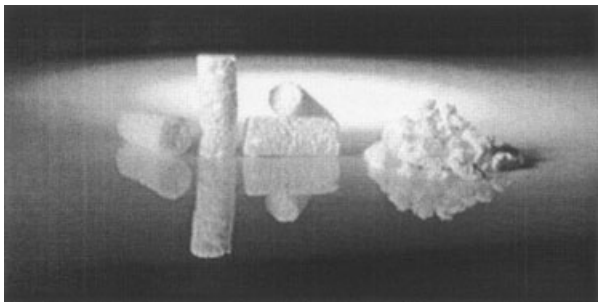

Figure 4. VITOSS, commercially available in block (left) or morsel (right) form.

1. hydrolysis/reesterification
2. (a) alcohol condensation/hydrolysis (b) water condensation/hydrolysis
3. gelation
4. densification

The rate of sol-gel reactions is dependent upon the strength and concentration of the acid used. The following scheme[2,57] can be exemplified:

1. Hydrolysis/reesterification: $Si(OC_2H_5)_4 + H_2O \leftrightarrow HO—Si(OC_2H_5)_{4-n} + nCH_3CH_2OH$ (where $n = 1–4$)
2. (a) Alcohol condensation/hydrolysis: $(OC_2H_5)_{4-n}Si—OH + Si(OC_2H_5)_4 \leftrightarrow (OC_2H_5)_{4-n}Si—O—Si(C_2H_5OH)_{4-n}$ (b) Water condensation/hydrolysis: $(OC_2H_5)_{4-n}Si—OH + (OC_2H_5)_{4-n}Si—OH' \leftrightarrow (OC_2H_5)_{4-n}Si—O—Si(OC_2H_5)'_{4-n} + H_2O$
3. Gelation: Cross linking of the silicon polymer continues and entraps solvent molecules, forming a porous matrix.
4. Densification: Collapse of the network causes shrinkage of the polymer and pores.

Typically, sol-gels prepared by acid catalysis will lose anywhere from 50–90% of their volume from removal of ethanol and other solvents.

The fluoroprobe employed in this study, 3-(4-carboxybenzoyl)quinoline-2-carboxyaldehyde (CBQCA), has been used extensively in capillary electrophoresis, where amino acids, peptides, and proteolyitic fragments were detected in the sub-attomolar ($< 10^{-18}$ M) range.[58] CBQCA possesses a broad dynamic range, and reacts exclusively with the primary

TABLE I. Compilation of the Various Properties of VITOSS Compared with Hydroxyapatite-Calcium Carbonate.

	VITOSS	*Hydroxyapatite-calcium carbonate*
Dose form(s)	Blocks (9 × 23 mm) Morsels (1–4 mm)	Morsels (1–4 mm)
Mineral phase(s)	β-tricalcium phosphate $Ca_3(PO_4)_2$	Hydroxyapatite Ca_{10} $(PO_4)_6$ (OH) calcium carbonate $CaCO_3$
Physical structure	Trabecular structure, polyporosity similar to cancellous bone	Porous structure, narrow pore size range
Porosity	Approximately 90%	Approximately 55%
Pore size (range)	1–1000 μm	280–779 μm
Resorption	76% at 6 weeks 86% at 12 weeks	20% at 6 weeks 45% at 12 weeks
Ratio of bone in implant to adjacent bone (bone remodeling)	0.6 at 6 weeks (morsels) 1.2 at 12 weeks (morsels)	0.4 at 6 weeks 0.5 at 12 weeks
Blood/marrow absorption	Rapid & effective due to porosity range 90% interconnected pores	Lower porosity results in less absorption
Packing	Holds 3X its volume in fluid, blood/marrow	Less likely to hold fluid due to less porosity and larger average

amine functionalities present in aminoglycoside antibiotics, aminated sugars, proteins, and lipoproteins.[58–60] It is intrinsically nonfluorescent, yet generates a highly fluorescent derivative upon conjugation with primary amines in the presence of cyanide or thiols and is compatible with most low-concentration buffers. The derivatization reaction starts with the nucleophilic attack of cyanide on CBQCA, and then the amine group is incorporated and participates in the formation of a quinoline ring.[60] The reaction scheme of the derivatization between CBQCA and aminoglycoside antibiotics is illustrated in Figure 5. The CBQCA–antibiotic conjugate excites and emits at approximately 460 and 550 nm, respectively, which is evident in the peaks of the fluorometric spectra contained in Figure 6. Derivatization with a fluoroprobe is a feasible approach for antibiotic determination because tobramycin is the only molecule possessing primary amine functionalities to be found in the eluent bath. Fluorometry uses absolute intensity measurements rather than separation/detection; hence, separation is rendered unnecessary. 2-hydroxyl-1-napthaldehyde and fluorescamine are commonly used as fluorogenic agents for the determination of aminoglycoside antibiotics, namely, tobramycin.[61] Numerous procedures, such as capillary electrophoresis, polarography, chromatography, and mass spectrometry, are available for antibiotic determination; however, official methods usually involve microbiological procedures.[58,61] One method proposed for antibiotic detection[58,62] is the *o*-phthaldialdehyde (OPA) method by UV-VIS spectroscopy (λ max = 331 nm) to form an aminoglycoside-*o*-phthaldialdehyde complex. However, most studies in the literature chose various fluorometric techniques due to their high sensitivity and specificity over nonfluorescent techniques.

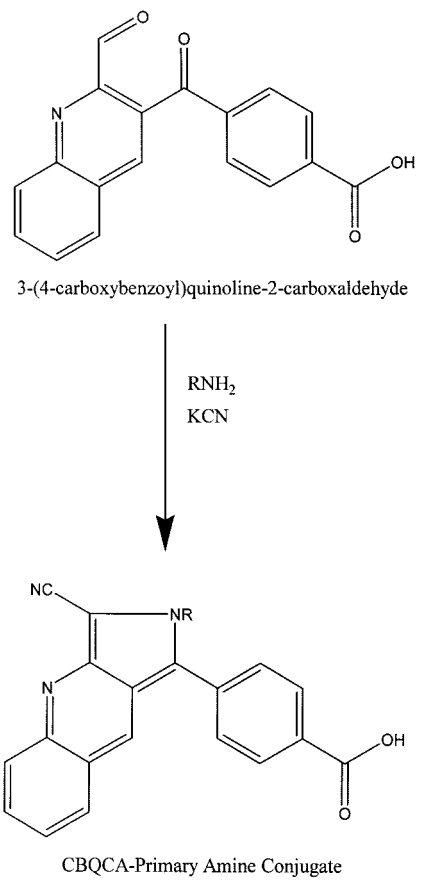

Figure 5. Chemical structure of CBQCA, including reaction scheme with aminoglycoside antibiotics.

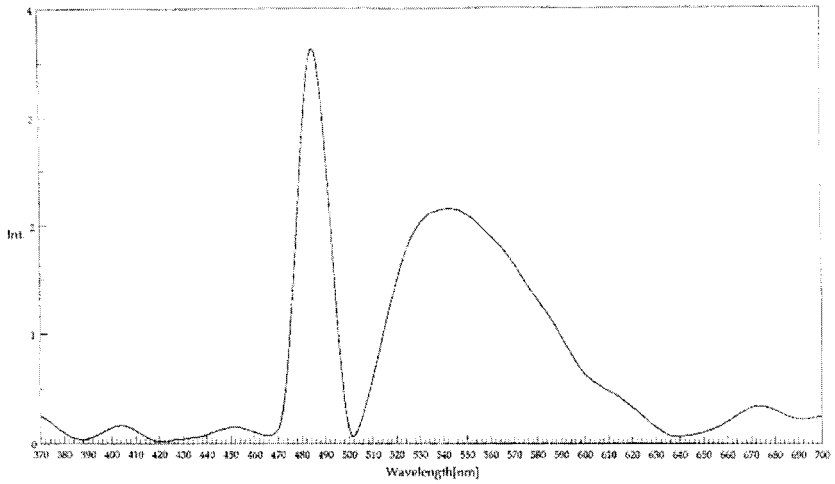

Figure 6. Fluorometric spectra of a derivatized CBQCA-tobramycin complex with characteristic excitation and emission peaks (460 and 550 nm, respectively).

METHODS

Methods Validation

Fluorescent intensities increased substantially after addition of several milligrams of tobramycin to the most concentrated standard solution assay, leading to the conclusion that at least sixfold molar excess of CBQCA [10 millimol/l (mM)] with a fivefold molar excess of potassium cyanide (KCN), a derivatization catalyst (10 mM), is sufficient to derivatize all antibiotic molecules present in the eluent assays. This was necessary because each tobramycin molecule reacts with up to five CBQCA molecules, as it possesses five reactive primary amine functional groups. A series of five standard solutions ranging from 0.01 ppm [10 parts per billion (ppb)] to 10.53 ppm were prepared from a stock solution of approximately 200 ppm tobramycin in PBS, which generated a reliable standard curve (refer to Figure 7). Tobramycin possessed an activity of 691 μg per 1000 μg and is complexed with sulfate $(SO_4)^{2-}$ in a 1:1.5 molar ratio. This stoichiometry was adjusted for prior to preparations of tobramycin standards and loading. A 2-h incubation period was sufficient for complete derivatization. Blanks from the PBS and CBQCA mixtures were evaluated and revealed near-zero intensity readings. The limits of detection (LOD) and limits of quantification (LOQ) concentration values have been established and were approximately one order of magnitude lower than the least concentrated standard.

Materials Preparation and Derivatization

Protocols for the acid-catalyzed synthesis of silicate xerogel were conducted according to the following procedures:[51–53]

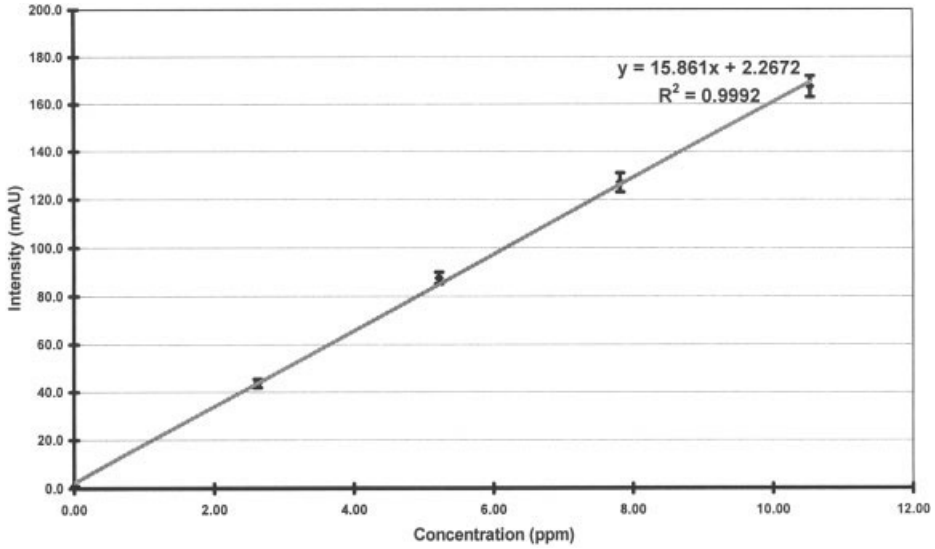

Figure 7. Linear fluorescence standard curve used to determine tobramycin elution concentration (AU—arbitrary units).

TABLE II. Brief Descriptions for the Various VITOSS-Silicate Xerogel Systems, VITOSS Studies VS1–VS5.

	VITOSS Study VS1	VITOSS Study VS2	VITOSS Study VS3	VITOSS Study VS4	VITOSS Study VS5*
Description	VITOSS block; tobramycin impregnated; non-silicate xerogel encapsulation	VITOSS block; tobramycin impregnated; non-silicate xerogel encapsulation	VITOSS block; tobramycin impregnated; silicate xerogel encapsulation	VITOSS block; tobramycin impregnated; silicate xerogel encapsulation	VITOSS block; tobramycin impregnated directly into silicate xerogel encapsulation
Loaded silicate xerogel mass (g)	0.0	0.0	0.1655	0.1445	0.3229
Silicate xerogel: VITOSS (w/w%)	0.0	0.0	~43 (42.98)	~36 (35.75)	~87 (87.04)

* For Study VS5, tobramycin was directly impregnated into silicate xerogel in which a VITOSS block was encapsulated.

Approximately 7.55 g TEOS (0.0360 mol) was combined with approximately 1.80 g 0.2 M HCl (0.00360 mol) and dissolved in 5.19 g THF (0.0720 mol) in a beaker. The resulting mixture was stirred with a magnetic stir bar and allowed to react for 1.5 h until it became viscous, at which time the stirring was discontinued. A clear sol-gel was obtained at this point.

Six VITOSS blocks with uniform masses, ranging from 0.3086 to 0.4042 g, were carefully selected. Each block was visually inspected and was free of voids, fractures, fissures, or any other morphological abnormalities. Four VITOSS blocks were impregnated with tobramycin: two VITOSS blocks without silicate-xerogel encapsulation (designated as VITOSS Studies VS1 and VS2) and two VITOSS blocks with silicate-xerogel encapsulation (designated as VITOSS Studies VS3 and VS4). One VITOSS block was reserved for impregnating tobramycin directly into the silicate-xerogel encapsulation around it (designated as VITOSS Study VS5), in order to assess its particular elution characteristic. Additionally, one VITOSS block, which was encapsulated with silicate xerogel and not impregnated with tobramycin, served as the control. Brief descriptions for the various VITOSS/silicate-xerogel systems encompassed in this analysis, VITOSS Studies VS1–VS5, including silicate-xerogel encapsulation masses and silicate xerogel: VITOSS weight/weight percent (w/w%) ratios, are contained in Table II. The procedure for impregnating VITOSS with tobramycin entails the following scheme: Four solutions consisting of approximately 0.1310 g tobramycin dissolved into ~10 ml (~9000 ppm) deionized water were prepared. One VITOSS block was immersed into each of the four solutions for 24 h, allowing for maximum absorption/wicking of dissolved tobramycin into the inner pores of VITOSS. The VITOSS blocks were carefully removed from the solutions and placed onto a watch glass and into a drying oven at 37 °C for 24 h in order to evaporate the water, leaving tobramycin behind in the interstices of VITOSS. The loading masses of tobramycin were determined by subtracting the initial mass of the VITOSS blocks from the tobramycin-impregnated VITOSS masses.

The viscous silicate sol-gel solution (prepared on the same day when the VITOSS blocks were removed from drying) was then slowly poured onto two tobramycin-impregnated VITOSS blocks on a small watch glass. A minimal volume (~3–4 ml) of the silicate sol-gel was used in order to assure a uniform, complete encapsulation around the VITOSS blocks and that no excessive silicate would carry off any dissolved tobramycin through unwanted dripping. The silicate-encapsulated VITOSS blocks were then allowed sit for 24 h at room temperature to allow for maximum wicking/encapsulation into the pores. Further drying in a drying oven at 37 °C for 24 h was then necessary to evaporate any residual water and ethanol byproducts produced from the silicate sol-gel synthesis. Finally, 0.05 g tobramycin was used to impregnate a portion (~3.63 g) of the remaining silicate sol-gel solution. The mixture was stirred with a magnetic stir bar until the tobramycin completely dissolved. Immediately, a minimal volume (~3–4 ml) of the tobramycin-impregnated silicate sol-gel was then slowly poured onto a nonimpregnated VITOSS block on a small watch glass. The tobramycin-impregnated silicate-encapsulated VITOSS block was then allowed sit for 24 h at room temperature to allow for maximum wicking/encapsulation into its pores. Further drying was completed in a drying oven at 37 °C for 24 h in order to evaporate any residual water and ethanol. The encapsulation masses of silicate xerogel were determined by subtracting the initial mass of the VITOSS blocks from the silicate-xerogel-encapsulated VITOSS masses. The loading mass for tobramycin in the silicate xerogel was determined through a fraction of the volume of silicate xerogel absorbed by the VITOSS block. Silicate-xerogel-encapsulated VITOSS blocks exhibited a glossy appearance on its surfaces compared to non-silicate-xerogel-encapsulated VITOSS blocks.

Each of the six VITOSS blocks were immersed into six light-impervious containers containing 45 ml PBS at pH 7.0 that was previously heated to 37 °C and stored in a dark oven programmed at 37 °C (to mimic *in vivo* conditions). One hundred-microliter (μl) samples from each of the six elution baths were extracted daily with the PBS refreshed daily. The daily eluent samples were stored in microvials and refriger-

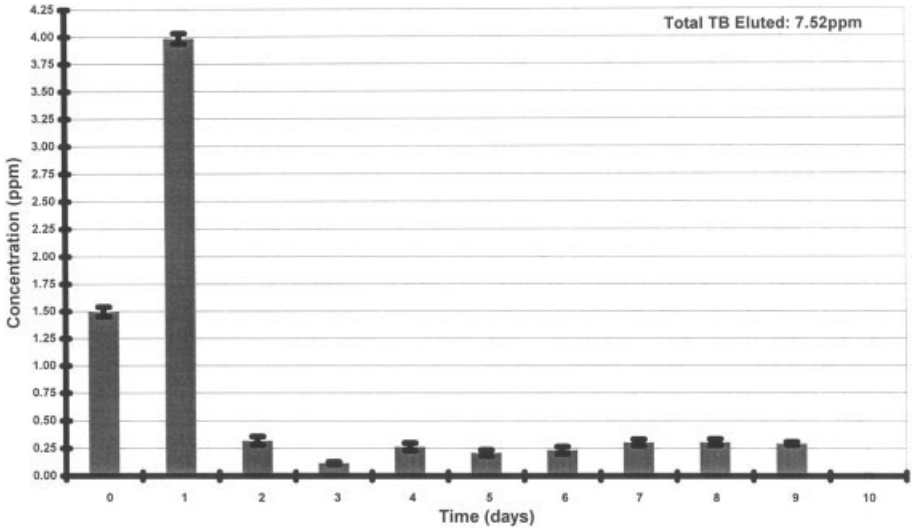

Figure 8. Daily elution profile of tobramycin from non-silicate-encapsulated VITOSS, Study VS1.

ated at −20 °C during the duration of the daily extractions. When the samples were thawed for derivatization and analysis, 100 μl of a 208.43 ppm tobramycin standard solution was prepared to generate the standard curves. Solutions of 26.75 μl CBQCA and 53.50 μl KCN were then added to all the daily eluent samples and the standard solution, yielding a total reaction volume of 180.25 μl. These derivatized mixtures were incubated for 2 h in dark conditions while the microvials were gently swirled every 15 min to allow for complete derivatization of the antibiotics. The derivatized reaction mixtures were then diluted with 1.8198 ml PBS to bring the final volume of the reaction mixture to precisely 2.000 ml. Dilution serves two purposes: It ceases any further derivatization and it brings the derivatized antibiotic concentrations within the range of medium to low intensity sensitivity on the fluorometer. Moreover, dilution was obligatory in order to fill the standard spectrometer cuvette (maximum volume of 4 ml) with a volume greater than 2 ml, the volume required for detection. Standard solutions were prepared with the use of the standard addition method by adding subsequent portions of PBS, which ranged in volume, to the cuvette to generate five concentrations/data points for the standard curve. Depending on the concentration of the antibiotics, eluent samples were further diluted until the antibiotics were within the detectable range of the standard curve. Each of the eluent samples, standards, and blanks were scanned five (n = 5) times. The unknown antibiotic concentrations were determined by comparing fluorescent intensity values to the standards of known concentration. Reported values were given as a mean from the five scans with their standard deviations (SD).

Statistical analysis for data variance was realized by utilizing the Student's t-test: two samples, assuming equal variance ($p < .05$ at 95% confidence limit), provided by Microsoft EXCEL® Software Data Analysis Toolpak.

RESULTS

The daily elution profiles of tobramycin from the various VITOSS studies, Studies VS1–VS5, illustrated in Figures 8–12, clearly indicate that tobramycin elution quantities markedly decrease, reaching a steady state within several days after the initial rapid concentrated elution from the scaffold network during the first few days. For all the studies, tobramycin elution from VITOSS was not detectable after Day 11. Figures 8 and 9 depict the elution characteristics of non-silicate-xerogel-encapsulated VITOSS, Studies VS1 and VS2, respectively. Tobramycin release was detected immediately after soaking, but the most concentrated burst of release was observed after 24 h of soaking (Day 1) for both studies. A total of 7.52 ppm tobramycin eluted during the duration of the 10-day study for Study VS1. For Study VS2, a replicate study of non-silicate-xerogel-encapsulated VITOSS, a total of 25.32 ppm tobramycin eluted in the allotted study time. This elution quantity is approximately three times greater than Study VS1; nevertheless, it is congruent, because Study VS2 was loaded with approximately three times greater tobramycin quantities compared to Study VS1. Figures 10 and 11 represent the elution characteristics of the silicate-xerogel-encapsulated VITOSS, Studies VS3 and VS4, respectively. Tobramycin release was detected instantaneously after soaking, with the most concentrated release burst occurring before Day 1 for both studies. A total of 108.08 ppm tobramycin eluted during the duration of the 10-day study for Study VS3. For Study VS4, a replicate study of silicate-xerogel-encapsulated VITOSS, a total of 133.20 ppm tobramycin eluted in the allotted study time. These elution quantities are virtually similar, as both Studies VS3 and VS4 were loaded with approximately the same quantities of tobramycin. Figure 12 shows the elution characteristics of tobramycin-loaded silicate-xerogel encapsulated VITOSS, Study VS5. Tobramycin release was detected immediately after soaking,

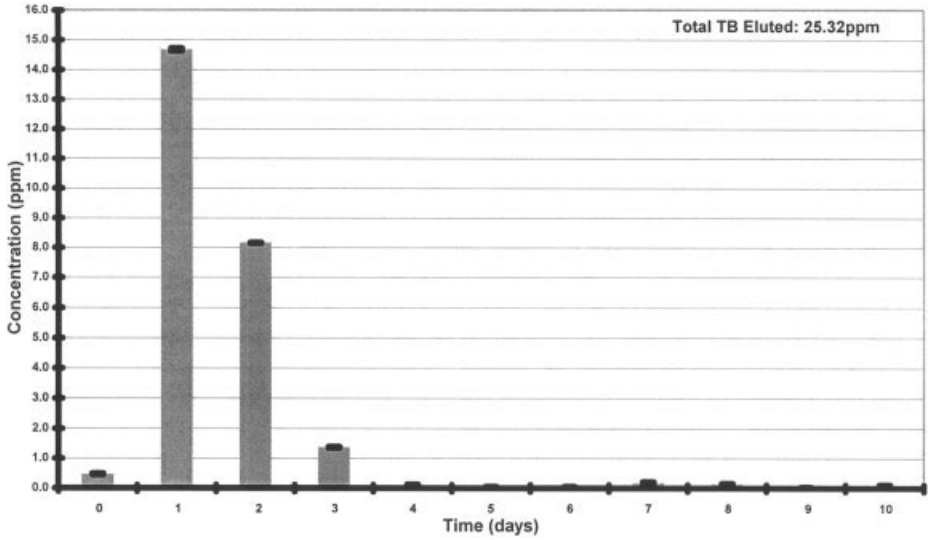

Figure 9. Daily elution profile of tobramycin from non-silicate-encapsulated VITOSS, Study VS2.

but the most concentrated burst of release was observed at Day 1 for this study. This elution behavior was reasonably analogous to the elution behavior described for non-silicate-xerogel-encapsulated VITOSS, Studies VS1 and VS2. A total of 46.61 ppm tobramycin eluted during the duration of the 10-day study for Study VS5. Despite the fact that the studies entailed different parameters and different tobramycin release quantities, they generally appeared to follow the same theoretical elution behavior, an exponential-decay-type release profile. Finally, the control study, consisting of silicate-xerogel–encapsulated VITOSS impregnated with no tobramycin, possessed absolutely zero fluorescence artifacts, thereby underpinning the specificity of the detection method.

The cumulative elution profile as a function of percent of loaded tobramycin eluted from the various VITOSS studies are depicted in Figure 13. A comparison of the data from the non-silicate-xerogel–encapsulated VITOSS (Studies VS1 and VS2) versus the data from the silicate-xerogel–encapsulated VITOSS (Studies VS3 and VS4) indicate that their elution profiles are drastically dissimilar, whereas comparison of the data obtained from replicating the respective studies suggest that they are consistent and somewhat equivocal. Studies VS1 and VS2 eluted 21.53 and 23.60% of loaded tobramycin, respectively, whereas Studies VS3 and VS4 eluted 60.65 and 61.31% of loaded tobramycin, respectively. Apparently, Figure 13 reveals that there is substantially greater overall elution of tobramycin from silicate-xerogel-encapsulated VITOSS compared to non-silicate-xerogel-encapsulated VITOSS in the time period elapsed. The exception, however, is Study VS5, where tobramycin-loaded silicate-xerogel-encapsulated VITOSS appeared to possess an elution profile similar to Studies VS1 and VS2, with 22.36%

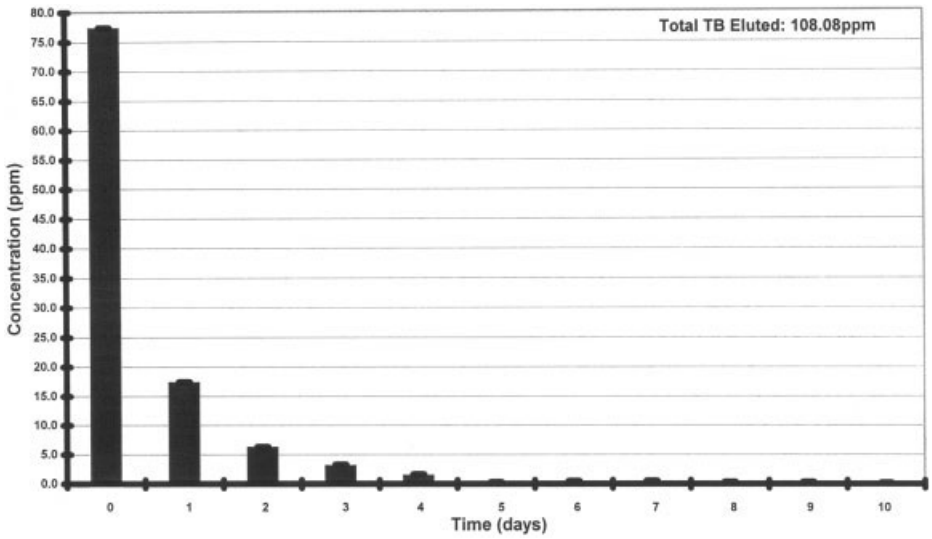

Figure 10. Daily elution profile of tobramycin from silicate-encapsulated VITOSS, Study VS3.

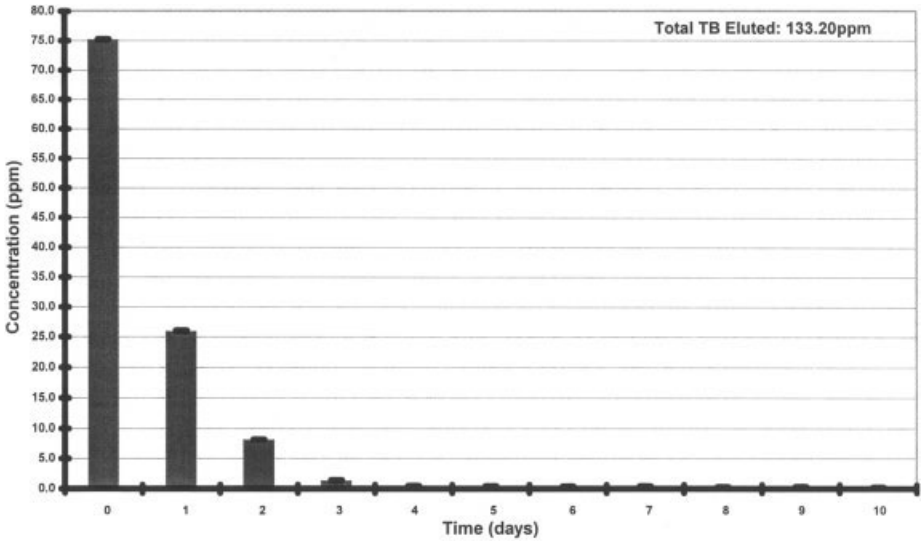

Figure 11. Daily elution profile of tobramycin from silicate-encapsulated VITOSS, Study VS4.

of loaded tobramycin eluted. The percent elution profiles of Studies VS1-VS5 behave linearly to a degree, indicating that tobramycin elution occurs in a moderate and steady fashion. Daily percent elution quantities were calculated from a ratio of the sum of the concentrations of tobramycin that were eluted daily over the total quantity of tobramycin loaded into VITOSS. The equilibration of data points at the end of the tobramycin analysis in Figure 13 were a result of the sample intensities being approximately equal to control intensities, which possessed virtually zero fluorescence. This behavior indicates that tobramycin elution was not detectable after the allotted time period for Studies VS1–VS5 (Days 10 and 11). After these data points, control and blank intensities were essentially equal to sample intensities, resulting in near-zero concentrations of tobramycin. Therefore, the flattening out of the curves at the end of the elution periods for the various studies point to the fact that tobramycin elution has vastly diminished and reaches a steady state.

Figures 14 and 15 provide a visual representation of total tobramycin eluted in micrograms and total tobramycin percent eluted for the VITOSS studies, respectively. Furthermore, the results from the Student's t-test have been summarized and are explicitly conveyed with respect to each study. Statistical results were rather stringent, perhaps due to the fact that data acquired possessed minimum SD and that various parameters encompassed the studies, collectively. Ironically, the exception lies between two different studies being statistically insignificant ($p = 0.069$), Studies VS1 and VS5, which have been previously demonstrated to have similar tobramycin elution percentages.

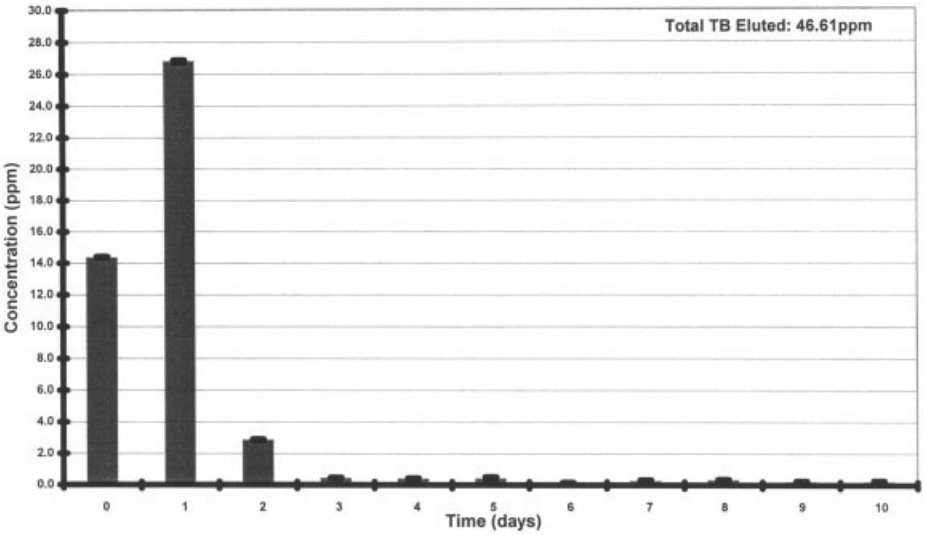

Figure 12. Daily elution profile of tobramycin from tobramycin-impregnated silicate-encapsulated VITOSS, Study VS5.

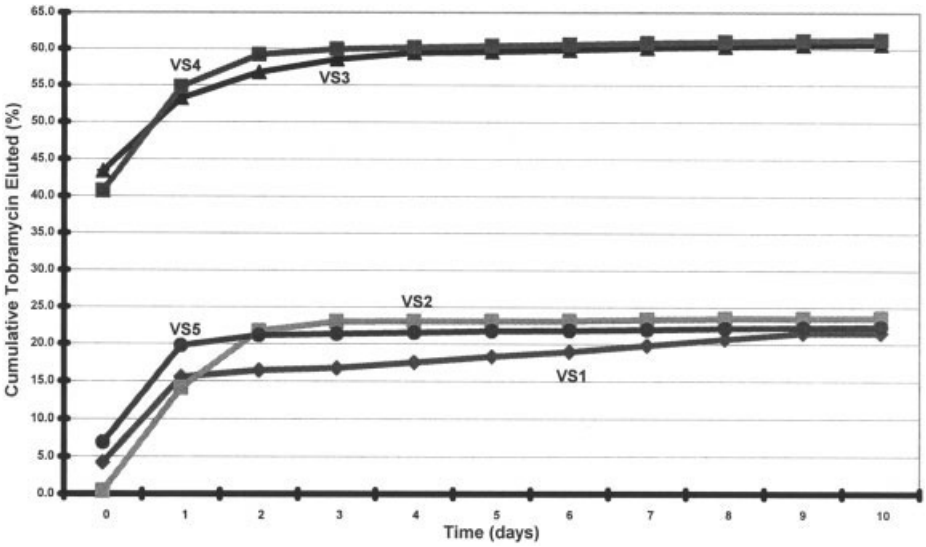

Figure 13. Cumulative percent elution profiles of tobramycin from VITOSS Studies VS1–VS5.

Figures 16 and 17 demonstrate Higuchi plots for tobramycin elution from the various VITOSS studies against the square root of time, expressed both as a function of cumulative micrograms of tobramycin eluted and cumulative percent of tobramycin eluted, respectively. Higuchi plots were constructed in order to reveal whether antibiotic release rates are linear or not over specific durations in an elution study. Tobramycin release rates for the entire studies were linear at the initial release stage on the plots (Days 0–3). However, tobramycin release rates were remarkably reduced after 3 days in the latter release stages on the plots (Days 4–10), while reasonably adhering to a linear fashion. These results suggest that tobramycin release from the entire studies occurs in a consistent, steady manner. Additionally, various elution characteristics and trends observed for a specific study in the previous plots are evident here in Figures 16 and 17. To specify, Study VS1 seemed to possess the least trend uniformity in the latter tobramycin release stages when compared to all the studies, and this can be visualized prominently in Figure 8, Days 4–10.

Figures 18 and 19 contain log plots for cumulative micrograms of tobramycin eluted and cumulative percent of tobramycin eluted from the various VITOSS studies, respectively. Log plots of concentrations were constructed in order to realize qualitatively the kinetics of antibiotic release and to quantitatively acquire first- and zero-order rate constants from the initial and latter slopes, respectively. These slopes are directly proportional to tobramycin release rates and furthermore, larger slopes point to those VITOSS studies yielding greater tobramycin release concentrations. It is evident from the plots that Study VS2 possessed the largest slope, whereas Studies VS3 and VS4 possessed the smallest

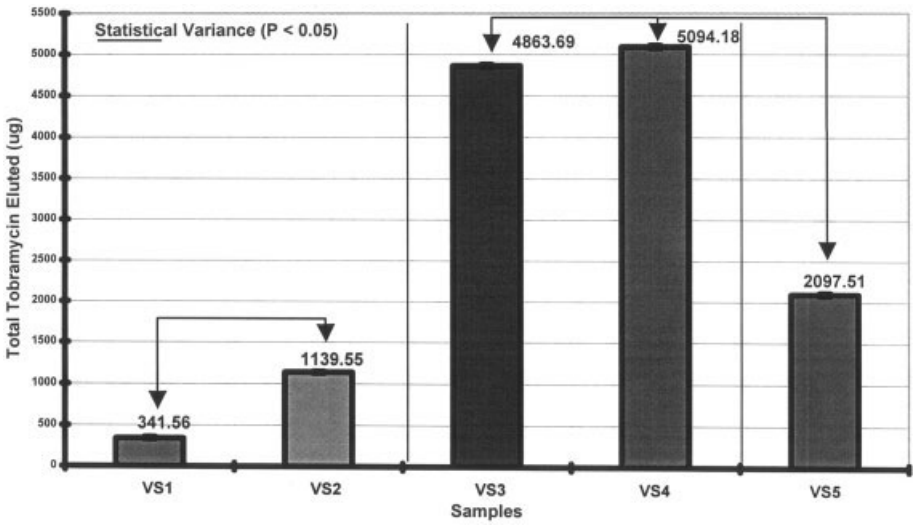

Figure 14. Bar-graph representation of total micrograms of tobramycin eluted from VITOSS Studies VS1–VS5, including statistical summary from Student's t-test.

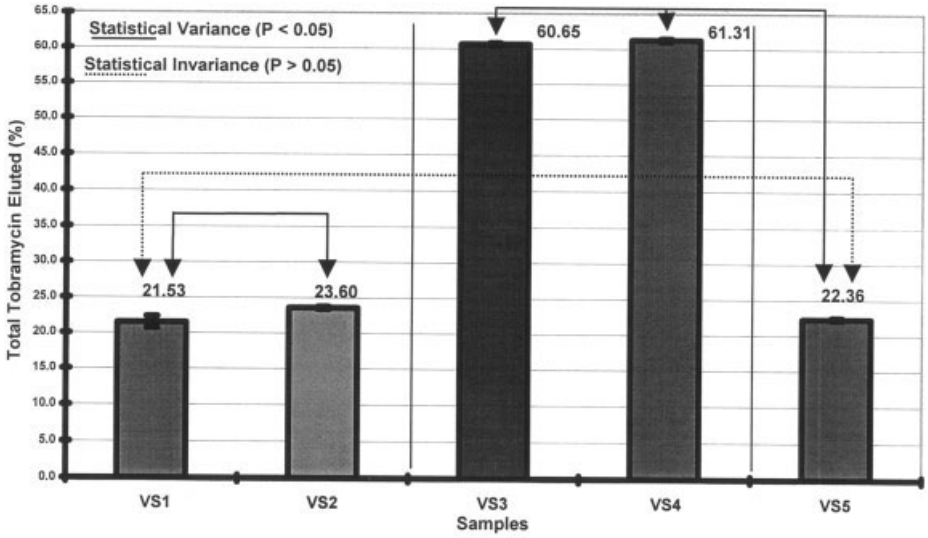

Figure 15. Bar-graph representation of total percent tobramycin eluted from VITOSS Studies VS1–VS5, including statistical summary from Student's t-test.

slopes. The slopes of Studies VS1 and VS5 were intermediate and seemed analogous in comparison with each other. Tobramycin release rates for all the studies were linear and first order at the initial release stage on the plots. However, the slopes for the tobramycin release rates were reduced, and approached zero after 3 days, implying that zero-order kinetics were predominant in the latter release stages after transitioning through a pseudo-first-order rate release stage occurring approximately around Days 2 and 3.

Table III contains a quantitative summary of least-squares-method operations on the initial and latter tobramycin release stages obtained from the Higuchi plots and of the first- and zero-order rate constants of the initial and latter tobramycin release stages derived from the log plots, respectively, for the various VITOSS studies. The R values for the initial tobramycin release stage for VITOSS Studies VS1 and VS5 and the latter release stage for Study VS2 deviate slightly from linearity, which is clearly observed from the Higuchi plots in Figure 16 and 17. This may be attributed to these studies displaying a less smooth slope transition occurring from first- to zero-order rate kinetics around Days 2 and 3 as compared to VITOSS Studies VS3 and VS4. As can be seen from the slopes of the log plots in Figures 18 and 19, Study VS2 possessed the highest first-order rate constant, whereas Studies VS3 and VS4 possessed the smallest first-order rate constants. Again, the first-order rate constants from Studies VS1 and VS5 were comparable. These results show that tobramycin release rates were a function of the physical characteristics of a specific VITOSS study. In addition, initial tobramycin elution first-order rate constants were proportional to the

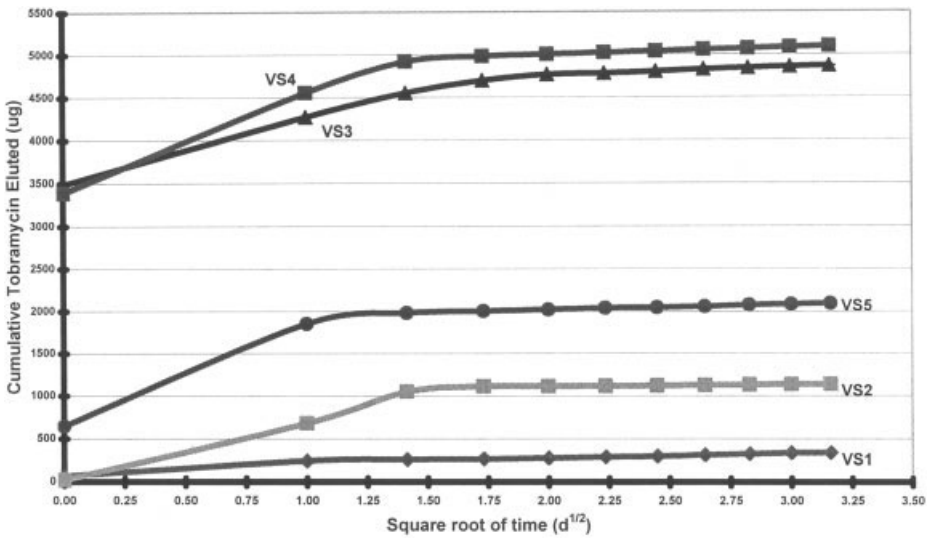

Figure 16. Higuchi plots for cumulative micrograms of tobramycin eluted from VITOSS Studies VS1–VS5.

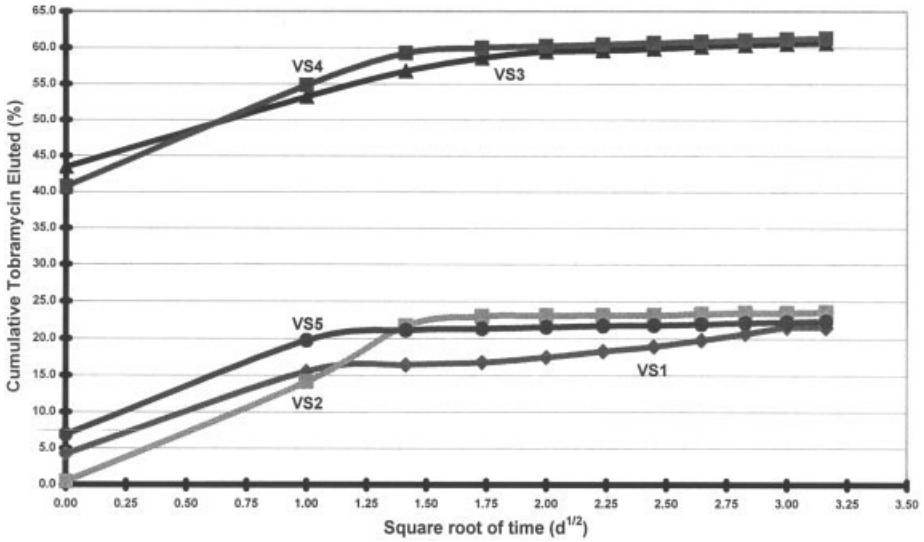

Figure 17. Higuchi plots for cumulative percent tobramycin eluted from VITOSS Studies VS1–VS5.

quantity of tobramycin loaded into the various VITOSS studies (comparing Study VS1 with VS2 and comparing VS3 with VS4).

Table IV summarizes the relevant data and parameters associated with the tobramycin-impregnated silicate-encapsulated VITOSS studies. VITOSS block masses, tobramycin, VITOSS w/w% ratios, average tobramycin eluted per day, and error associated with respective studies have been reported. Total tobramycin elution percents were determined by dividing total quantities of tobramycin in parts per million by the quantity of tobramycin loaded in grams converted into micrograms multiplied by 45 ml volume of PBS and then 100. Tobramycin elution quantities, concentrations, and percentages were directly proportional to the quantities of tobramycin that were impregnated in the VITOSS blocks at the time of delivery for Studies VS1–VS4. Loading/elution proportionality was not a principal concern of this work, but these results do support findings in the literature,[6,22] stressing that antibiotic release rates increased with increasing antibiotic quantity concentration and that varying the quantity of antibiotic in the bone cements can control release rates. However, no proportionality exists between VITOSS Study VS5 and Studies VS1–VS4, due to the media differences for encapsulating tobramycin. The results reported herein were representation data from four separate trials possessing variations of $<4\%$.

DISCUSSION

According to the Higuchi plots, diffusion-controlled antibiotic release from a matrix-type drug delivery system such as

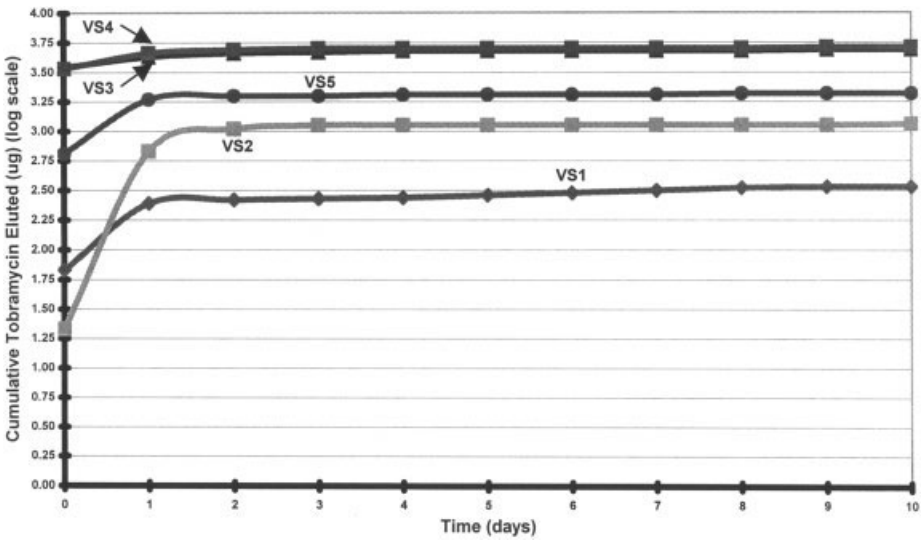

Figure 18. Log plots of cumulative micrograms of tobramycin eluted from VITOSS Studies VS1–VS5.

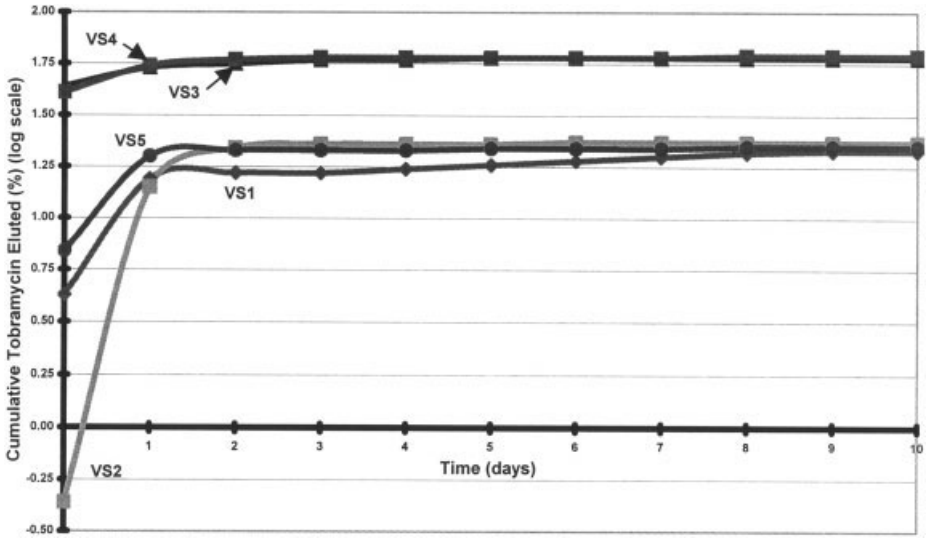

Figure 19. Log plots of cumulative percent tobramycin eluted from VITOSS Studies VS1–VS5.

silicate-xerogel-encapsulated VITOSS blocks typically are linearly correlated with the square root of time. Tobramycin release from the matrix blocks can be generally expressed through the Higuchi equation[63] [Eq. (1)]:

$$M_t = A\{[D_i \varepsilon C_s(2C_d - \varepsilon C_s)t]/\tau\}^{1/2} \quad (1)$$

where M_t is the antibiotic released from the cement at time t, A is the surface area of the cement tablet, D_i is the diffusivity of the antibiotic, C_s is the solubility, C_d is the concentration of the antibiotic, τ is the tortuosity, and ϵ is the porosity of the cement. The tobramycin elution profiles of Studies VS1–VS5 in the Higuchi plots were linear at the initial and latter stages in the plot, assuming that the rate-limiting step of release was the tobramycin diffusion process in the micropores of VITOSS. However, the release profiles show a reduction in tobramycin release rates with a slight deviation in linearity at the pseudo-first-order rate release stage transition occurring around Days 2 and 3. This suggests that the geometrical structure of the VITOSS pores may have been altered in the latter stages of the tobramycin elution analysis by biodegradation and/or precipitation/formation of hydroxyapatite, which has been previously confirmed through FTIR analysis.[2]

The tobramycin elution profiles of Studies VS1–VS5 in the log plots were linear at the initial stages in the plot with large positive slopes, indicating that the initial tobramycin release adheres to first-order rate kinetics. Simply stated, a first-order rate of release signifies that the rate of tobramycin elution is directly dependent on the concentration of tobramycin present in the VITOSS matrix at any given instance. Tobramycin elution levels will decrease as a direct result of fewer tobramycin molecules present in VITOSS. Therefore, the tobramycin elution profiles generally should possess the shape of an exponential-type decay curve, which can be visualized from tracing the graphs contained in Figures 8–12. For the latter tobramycin release stages in the log plots where the slopes are near zero, the changing concentration of tobramycin in the VITOSS matrix does not change the rate of tobramycin elution, thus adhering to zero-order rate kinetics.[64] Here in the latter zero-order kinetics release stage, zero-order rate constants are very small and approach zero. It

TABLE III. Summary of Least-Squares Method Operations Obtained from the Initial (Days 0–3) and Latter (Days 4–10) Tobramycin Release Stages in the Higuchi Plots, and First- and Zero-Order Rate Constants Obtained from the Initial and Latter Tobramycin Release Stages in the Log Plots, Respectively, for VITOSS Studies VS1–VS5.

	VS1: Non-Silicate Encapsulated	*VS2: Non-Silicate Encapsulated*	*VS3: Silicate Encapsulated*	*VS4: Silicate Encapsulated*	*VS5: Silicate Encapsulated**
R value; Initial stage in Higuchi models (conc. vs. time$^{1/2}$)	0.9477	0.9924	0.9964	0.9836	0.9509
R value; Latter stage in Higuchi models (conc. vs. time$^{1/2}$)	0.9921	0.9761	0.9957	0.9997	0.9962
First-order rate constant, k (day^{-1})	0.76	1.38	0.74	0.75	0.81
Zero-order rate constant, k (day^{-1})	0.0157	0.0011	0.0018	0.0018	0.0021

* For Study VS5, tobramycin was directly impregnated into silicate xerogel in which a VITOSS block was encapsulated.

TABLE IV. Summary of relevant data and parameters for Tobramycin-impregnated VITOSS with silicate xerogel, Studies VS1–VS5.

	VS1: Non-Silicate Encapsulated	*VS2: Non-Silicate Encapsulated*	*VS3: Silicate Encapsulated*	*VS4: Silicate Encapsulated*	*VS5: Silicate Encapsulated**
VITOSS mass (g)	0.3269	0.3086	0.3851	0.4042	0.3710
Loaded tobramycin (μg)	1586.21	4827.59	8019.32	8309.18	9379.31
Tobramycin: VITOSS (w/w%)	~0.50 (0.49)	~1.50 (1.56)	~2.00 (2.08)	~2.00 (2.06)	2.82*
Total Tobramycin eluted (ppm)	7.52 ± 0.30	25.32 ± 0.21	108.08 ± 0.35	133.20 ± 0.40	46.61 ± 0.41
AVG Tobramycin eluted (ppm/day)	0.75 ± 0.03	2.53 ± 0.02	10.81 ± 0.04	13.32 ± 0.04	4.66 ± 0.04
Total Tobramycin eluted (μg)	341.56 ± 13.65	1139.55 ± 9.26	4863.69 ± 14.98	5094.18 ± 17.99	2097.51 ± 18.27
Total Tobramycin eluted (%)	21.53 ± 0.86	23.60 ± 0.19	60.65 ± 0.19	61.31 ± 0.22	22.36 ± 0.19
RSD (%)	3.99	0.81	0.31	0.36	0.85

* For Study VS5, tobramycin was directly impregnated into silicate xerogel in which a VITOSS block was encapsulated.

is also apparent that non-silicate-xerogel-encapsulated VITOSS (Study VS2) possessed the highest first-order rate constant (Table III). The most salient feature of this finding is that tobramycin diffusion is hindered only by the pores/micropores of VITOSS, as opposed to silicate-xerogel-encapsulated VITOSS (Studies VS3 and VS4) where tobramycin diffusion is obstructed by an additional xerogel barrier. The notably lower first-order rate constants for Studies VS3 and VS4 were anticipated and attested to this distinctiveness. One must also bear in mind that Studies VS3 and VS4 were also loaded with significantly greater quantities of tobramycin compared to Studies VS1 and VS2 (Table IV). If one neglects the fact that Study VS2 was loaded with approximately three times the quantity of tobramycin compared to Study VS1, all those studies that possessed only one barrier through which tobramycin diffused (Studies VS1, VS2, and VS5), whether it be silicate xerogel or just the interstices of VITOSS, possessed seemingly equivalent first-order rate constants. The twofold increase in the first-order rate constant for Study VS2 compared to Study VS1 verifies that the tobramycin release rates are directly dependent on tobramycin loading quantities. However, Study VS5, comprising the highest loading quantities of silicate xerogel (Table II) and tobramycin, which was impregnated into the silicate xerogel, released a significantly lesser quantity of tobramycin as compared to Studies VS3 and VS4, which also contained higher loading quantities of tobramycin. This result was envisaged because of the design properties of the silicate xerogel that was prepared. As stated previously, the pores of silicate xerogel can be altered to vary in size from macroporous to microporous. Previous characterizations attained from nitrogen adsorption porisiometry[2] have shown that the silicate xerogel was mesoporous and monodispersed (0.2–50.0 Å), with an average pore diameter of 32.6 Å. Mesoporosity can be ascribed to the fact that considerable quantities of tobramycin were dissolved in TEOS during its homopolymerization. Nonetheless, these pore sizes are considerably smaller than the micropores/pores of VITOSS (100 nm/200 μm) thus making it less permeable for tobramycin diffusion. In addition, silicate-xerogel matrix is slightly less hydrophilic than the VITOSS matrix. Speculatively, this could perhaps contribute to the observed lesser tobramycin elution quantity directly from the silicate xerogel. Studies VS3 and VS4 afforded the best overall tobramycin elution profiles from a percentage and controlled-release perspective in that they displayed an exponential-decay-type release idealistic of a uniform release mechanism. They clearly demonstrate a profound dependency on the tobramycin concentrations present in the VITOSS matrix at a given instance. Ultimately, these results advocate that tobramycin elution characteristics and release rates can be managed by varying the quantity of tobramycin in VITOSS and/or by encapsulation VITOSS with silicate xerogel.

Antibiotic release from bone cements is regulated by the extent of polar dissolution fluids penetrating beyond the surface and into the pores of the cement.[65,66] The magnitude of dissolution fluid penetration depends critically on the porosity and the wettability of the bone cement,[5] and is also governed by how well it contacts its surface. Porosity is directly related to the surface area of a bone cement, dictating its surface roughness, and therefore, the quantity of dissolution fluid that will contact its surface. Succinctly, greater porosity points to greater surface area, allowing more dissolution fluid to contact the bone cement thus enhancing antibiotic release. Wettability emulates surface roughness and the degree of hydrophilicity that bone cement possesses. The greater hydrophilicity bone cement possesses, the more likely dissolution fluid diffusion will occur. However, much debate has arisen concerning the poorly understood antibiotic release mechanism.[67] However, it has been suggested, that slight wear in the form of fissures, air pockets, surface roughness, etc. in the bone cement are necessary in order to permit antibiotic release, which basically shows it to be a surface-area effect. From this theory, many researchers agree that antibiotic release from bone cements is fundamentally a surface-chemistry phenomenon.[65,66] Correspondingly, in this analysis, tobramycin release is aided by the penetration of bodily fluids

beyond the surface interface and into the pores and micropores of VITOSS. Consequentially, the hydrophilicity of the matrix network of VITOSS will denote the extent of contact and migration of polar extracellular dissolution fluid that enters to solvate tobramycin. Equally, the hydrophilicity of an antibiotic itself is crucial to its dissolution capacity and must not be disregarded. Experimental evidence from a phase-partitioning study previously conducted[68] on tobramycin reinforces its potential for aqueous solubility. The calculated log P and equilibrium constant value (K) for tobramycin were $-$ 7.32 and 4.79×10^{-8}, respectively. The greater magnitude of the log P and K values reflects its high degree of hydrophilicity, which leads to easier distribution into the aqueous phase. Results stress that practically 100% of tobramycin remains in the aqueous phase and trace quantities of tobramycin may partition in nonpolar phases. Hence, tobramycin is highly hydrophilic, endowed with the capability to simultaneously disperse into the VITOSS/silicate-xerogel network and PBS, facilitating its dissolution and release. Other factors abet tobramycin elution quantities as well. Tobramycin elution may be enhanced by its complexation with five highly polar SO_4^{2-} salts. The incorporation of a salt in tandem in order to increase the polarity of tobramycin will significantly interact with the solution chemistry. The salt may concurrently assist tobramycin dissolution by interacting with various ions found in the PBS for complexation. This interaction of an antibiotic with similar miscible specie is favorable, because the integration of two or more water-soluble antibiotics into bone cement greatly boosts overall elution.[15] Pharmacokinetic data on gentamicin and vancomycin/PMMA systems support this postulation, as the antibiotics were undetectable in the urine after the tenth day of fixation.[69] Nevertheless, the presence of a salt could perhaps be responsible for greater elution quantities compared to just the free-base form of tobramycin. By and large, tobramycin release from VITOSS can then be viewed as a pooled effect resulting from its porosity, its surface characteristics,[5] its hydrophilicity, and intrinsic antibiotic solubility.

Tobramycin elution behavior reaches an initial maximum during the first 24 h followed by a steady, decreasing elution. The initial tobramycin release maximum is attributed to the dissolution of tobramycin molecules adsorbed[70] onto the VITOSS/silicate-xerogel surface or to the diffusion of tobramycin molecules close to the surface. Additionally, the initial maximum is ostensibly dependent upon the quantity of tobramycin that was loaded into VITOSS. This elution behavior is independent of bone cement type and has been reported previously.[5,6,62,71] Numerous citations[62,71] describe a fast initial release of antibiotics from cements during the first 10 h of soaking, which decreases substantially after the first 24–36 hours, followed by sustained release. Furthermore, antibiotic levels remained near the MIC, inhibiting bacteria growth for 7–10 days.[15,62,67,71] Other prevailing factors, namely fluid saturation, may play an additional role in the observed tobramycin elution characteristics. The continued, steady elution of tobramycin at or near equivalent levels up to the tenth day after impregnation may be phenomenological to specific solution chemistry. A plausible explanation for this is that tobramycin concentrations have achieved a state of hydrostatic equilibrium, which results from constantly refreshing a fixed quantity of PBS (at equally spaced intervals), making the rate of tobramycin dissolution equivalent to the rate of tobramycin recrystallization. This transpires as a result of water pressure (PBS) within the VITOSS/silicate xerogel directly solvating the tobramycin that is embedded in the matrix and tobramycin reversibly precipitating from the solution or material surface into the matrix. This precipitation/recrystallization effect is expected to be more prominent in a semistatic *in vitro* analysis where hydrostatic equilibrium is more likely to be attained. However, in a dynamic *in vivo* analysis, where bodily fluids are continuously refreshed and circulating, this process is pushed further in the direction of dissolution, making it more unlikely to establish hydrostatic equilibrium and promote tobramycin recrystallization. Nonetheless, in an *in vitro* analysis, this behavior is predicted to gradually diminish over the next several days, thus facilitating optimal release of tobramycin. Likewise, contributing to the observed tobramycin elution characteristics is hydroxyapatite crystals precipitating out of any PBS that could have evaporated and depositing on the VITOSS/silicate-xerogel surface via ionic interactions as a result of a high degree of saturation of salts. Consequentially, sample eluents were not further refreshed after Day 11 and the analyses were terminated, suggesting that the elution of the tobramycin approached zero concentration. Here, at lower detectable levels of tobramycin elution, concentrations loomed near the limit of quantification.

The progressive formation of a hydroxyapatite layer on the surface of bioactive VITOSS and silicate xerogel can also affect tobramycin elution characteristics in that it may inhibit the release of loaded tobramycin in the latter stages of the analysis. In essence, the primary release of the tobramycin occurs prior to the initial formation of the hydroxyapatite layer. Confirmation of the formation of a hydroxyapatite layer occurring approximately 7–9 days after soaking VITOSS in PBS has been verified previously[72] by utilizing Fourier-transform infrared spectroscopy (FTIR). The initial concentrated release of tobramycin from VITOSS is in accord with the Ca^{2+}—H_3O^+ ionic exchanges between VITOSS and the PBS, thus promoting further dissolution. This ionic exchange is catalyzed by the inherent alkalinity of VITOSS. It can be asserted that the mechanism for initial antibiotic release from bioactive bone cements is not completely diffusion controlled; rather, it is enhanced by the ionic exchanges with the surrounding environment.[62]

The unique surface reactivity of bioactive silicate xerogels plays a vital role in determining the extent of antibiotic elution. Over time, various reactions transpire *in vitro* and *in vivo* at the xerogel surface, with the initial ionic exchanges occurring purportedly in sequence. The first stage is the loss of acidic sites or hydrogen ions (H^+) from the surface of the silicate xerogel via ionic exchanges with sodium (Na^+), hydronium (H_3O^+), other various metallic cations (M^+), and hydroxide (^-OH) present in PBS.[73] This exchange occurs

quite rapidly, within minutes of material exposure to PBS or bodily fluids, and creates a dealkinization of the xerogel surface layer with a net negative surface charge. During these first minutes when a bioactive xerogel contacts PBS, the loss of H^+ causes a localized breakdown of the xerogel network with the resultant formation of silanol groups [$Si(OH)_4$], which then repolymerize into the silicate-rich surface layer. As a result, the surface becomes rather porous on a microscopic scale, with average pore sizes ranging from 30–50 Å.[73] Following the ion-exchange stage, an amorphous calcium phosphate or hydroxyapatite layer will form on the xerogel surface, enhancing bioactivity[74] by incorporating biologic moieties, for example, blood proteins, collagen, and osteoblasts. It has been previously shown[36,42] that partial substitution of TEOS with organomodified alkoxysilanes affects the degradation behavior of the silicate xerogel matrix *in vitro* in that the degradation rate decreased with an increasing quantity of alkoxy silanes used, reducing its ion-exchange potential because of the decreasing hydrophilic character of the matrix. In addition to this, silicate xerogels that possess high moisture content compared to xerogels that are dried to constant weight demonstrated a faster degradation rate because of a higher degree of hydrophilicity and discontinuation of the condensation reaction. However, degradation of the silicate-xerogel matrix during soaking in PBS can typically be gauged quantitatively by measuring dissolved $Si(OH)_4$ in the media as a molybdenum blue complex by UV-VIS spectroscopy at 820 nm,[42] but this was not of chief concern for this work. Titrations conducted prior[2] on nondoped sol-gel-derived silicate xerogels that were applied in this analysis established that there are two distinct acidic sites present, having a pK_a roughly equal to 4.0. These titration data confirm that at a physiological pH of 7.2, the acidic sites on the xerogel surface are deprotonated by interactions with ^-OH and other cations and anions present in PBS, affecting the microstructure morphology of the surface. With prolonged exposure to PBS, eventually more interior acidic sites in the silicate xerogel will be hydrolyzed, accentuating the biodegradability of the xerogel at physiological pH. Surface alteration of silicate xerogel through ionic exchanges with its environment allows tobramycin molecules to significantly interact with the various ions concomitantly, optimizing its release. This surface alteration suggests that pore diameter increases, perhaps permitting more PBS to migrate into the matrix, solvating more tobramycin, and shifting the dissolution equilibrium vastly to the right. This may be indicated by the inherent tobramycin elution characteristics of the silicate-xerogel-encapsulated VITOSS studies, where greater quantities of tobramycin are released initially when compared to the non-silicate-xerogel-encapsulated VITOSS studies. This effect, though, yields only a minor contribution because the initial release of tobramycin depends ultimately on its loading quantity.

The initial tobramycin elution maximum surveyed from the VITOSS studies affirms that optimal antimicrobial activity is most profound during the early stages of release and that tobramycin is delivered in longer-release dosages for at least 11 days, with total elution quantities exceeding conventional systemic routes. Tobramycin elution concentrations are projected to be above its MIC of 2–30 ppm/day[18] directly after implantation, thereby providing a high level of local antiseptic effects around the bone–VITOSS surface interface**.** Here**,** an initial burst of tobramycin release could actually be quite effective in eradicating the microorganisms at the infection site; later, lower release rates of tobramycin could be effective in maintaining a sterile medium.[27] Therefore, a direct, controllable, biodegradable drug-delivery system like tobramycin-impregnated VITOSS allows for an optimal drug-delivery system by delivering tobramycin levels appropriate for microbial growth inhibition. In addition, a modified system such as tobramycin-impregnated silicate-xerogel-encapsulated VITOSS, which released the largest initial and overall concentrations and percentages of tobramycin, has been demonstrated to have even greater efficacy in immediately reaching and sustaining the MIC levels, making it an outstanding entrant in the operating realm compared to tobramycin-impregnated VITOSS alone. Because the elution characteristics of hydrophilic tobramycin from silicate-xerogel-encapsulated VITOSS have been evaluated, a drug-delivery system like this can be exploited to include other hydrophilic antibiotics. Tobramycin is sufficiently hydrophilic with substantial elution potential from VITOSS, and a hybrid tobramycin-gentamicin/silicate-xerogel-encapsulated VITOSS delivery system would be advantageous because of favorable aqueous solubility. Moreover, a combination of tobramycin with a less hydrophilic antibiotic such as the peptide-based vancomycin can be employed to increase elution potential and widen the spectrum for microbial inhibition. As a final point, nonpolar alkyl side chains can be introduced into the silicate-xerogel structural backbone to increase its hydrophobicity and suitability to elute nonpolar antibiotics, namely, the quinoline-based, wide-spectrum Levaquin and Fluoraquin. The VITOSS/silicate-xerogel drug-delivery system is an appropriate model for numerous substances, including biological substrates (enzymes and pro-osteogenic cells for templating, etc.), and it is not solely limited to tobramycin or other aminoglycoside antibiotics, because silicate xerogels can be chemically and/or structurally tailored rather easily to have affinity for countless substances. Silicate-xerogel-encapsulated VITOSS is therefore a formidable candidate for controlled drug delivery and should compete well with established β-TCP and hydroxyapatite drug-delivery systems.

CONCLUSIONS

In recapitulation, approximately threefold greater elution quantities of tobramycin were detected from non-silicate-xerogel-encapsulated VITOSS Study VS2 when compared to the other non-silicate-xerogel-encapsulated VITOSS, Study VS1, stressing dependency on initial loading quantities. Similarly, silicate-xerogel-encapsulated VITOSS, Studies VS3 and VS4, which possessed approximately equivalent tobramycin loading quantities, eluted virtually similar quantities.

In the same light, the first-order rate constant for non-silicate-xerogel-encapsulated VITOSS Study VS2 was approximately twofold greater than Study VS1 and silicate-xerogel-encapsulated VITOSS, Studies VS3 and VS4, which possessed an additional diffusion barrier. Study VS5, where tobramycin was impregnated directly into the silicate-xerogel-encapsulated VITOSS, was most impervious to tobramycin elution as a consequence of it possessing the largest silicate-xerogel loading mass as well as the xerogel cross-linked matrix. All studies basically displayed Higuchi-type linear uniform release kinetics throughout the tobramycin elution periods, tapering into zero-order release kinetics behavior. The ubiquitous ultraporosity and intrinsic hydrophilicity of VITOSS, in tandem with or without silicate xerogel, has allowed for optimum release percentages of tobramycin, which exceeds antibiotic percentages typically retrieved[7] from the original incorporation into bone cements. This study exemplifies that composite hydrophilicity determines the extent of body fluids migrating into the composite and promoting release for this appreciably polar antibiotic. Tobramycin elution was also aided by its high degree of hydrophilicity. Nevertheless, the complexation of tobramycin with highly polar SO_4^{2-} salts is a prominent factor responsible for the observed elution characteristics, enhancing release potential from a hydrophobic environment. Tobramycin elution characteristics indicate that there is an initial release maximum during the first 24 h that diminishes gradually several days after impregnation from the VITOSS/silicate-xerogel system, behaving similarly to other antibiotics loaded into cements, which are released at high concentrations initially, and then decrease steadily over time.[5] Because VITOSS is bioactive, in due course it forms an apatite-like layer on its surface, so the initial concentrated release of tobramycin, buttressed by ionic exchanges between the ceramic and environment, occurs prior to the initial formation of this bioactive layer. Based on the results ascertained from this research, the incorporation of adequately polar antibiotics such as tobramycin into a hydrophilic, bioresorbable VITOSS affords optimal release of the antibiotic, thereby providing high local levels at the bone–VITOSS interface, where it is needed most. It was also learned that silicate xerogels are robust regarding the optimal release of tobramycin from VITOSS, as they release higher percentages of tobramycin with respect to initial loading quantities when compared to non-silicate-xerogel-encapsulated VITOSS and tobramycin-impregnated silicate-xerogel-encapsulated VITOSS. This finding is due wholly in part to the simultaneous ionic exchanges occurring between the silicate xerogel and environment during the initial stages of the elution period, thereby enhancing the hydrophilic nature of the media with ions that complex themselves with tobramycin that is embedded in the pores of VITOSS. In addition to the higher tobramycin release percentages observed from silicate-xerogel-encapsulated VITOSS, the lower first-order rate constants and uniform, predictable first-order-type exponential-decay release profiles lend support to the notion that sol-gel-derived silicate xerogels are an ideal material for implementing controlled release of tobramycin or other polar antibiotics. Furthermore, chemical and/or structural tailoring of the silicate xerogel enables suitability to elute nonpolar antibiotics and an affinity for incorporating numerous substances into the VITOSS/silicate-xerogel system. Over time, VITOSS and hydrophilic silicate xerogels, prepared via the sol-gel process, are entirely bioresorbable, thus allowing virtually all of the impregnated antibiotics to be released after implantation. As a result of its biodegradability, silicate-xerogel-encapsulated VITOSS implants require little or no invasive surgery for their removal compared to nonbiodegradable high-porosity bone cements. Moreover, this system is promising from a clinical efficacy standpoint in that the bioavailability of tobramycin is not compromised due to the elution process. In conclusion, VITOSS encapsulated with silicate xerogel would therefore make an excellent candidate for a dependable, controllable, biodegradable antibiotic delivery system providing antibiotic concentrations high enough and at durations long enough to combat the numerous microbes encountered during surgery.

REFERENCES

1. Available: http://www.opm.gov/feddata/retire/projections.asp
2. Goldfinger A. Silicate glass: A novel drug delivery system [thesis]. Philadelphia: Temple University; 2000.
3. Vasquez M. Osteomyelitis in children. Curr Opinion Pediatr 2002;14:112–115.
4. Sasaki S, Ishii Y. Apatite cement containing antibiotics: Efficacy in treating experimental osteomyelitis. J Orthop Sci 1999; 4:361–369.
5. van de Belt H, Neut D, Uges DRA, Schenk W, van Horn JR, van der Mei HC, Busscher HJ. Surface roughness, porosity, and wettability of Gentamycin-loaded bone cements and their antibiotic release. Biomaterials 2000;21:1981–1987.
6. Richelsoph KC, Petersen DW, Haggard WO, Grisoni BF, Morris LH. Elution characteristics of tobramycin-impregnated medical grade calcium sulfate hemihydrate. In: 44th Annual Meeting, ORS; 1998 March 16–19; New Orleans, LA.
7. Poelestra KA, Busscher HJ, Schenk W, van Horn JR, van der Mei HC. Effect of Gentamycin loaded PMMA bone cement on *Staphylococcus aureus* biofilm formation. Biofouling 1999;14: 249–254.
8. Thomazeau H, Langlais F. Antibiotic release by tricalcic phosphate bone implantation. *In vitro* and *in vivo* pharmacokinetics of different galenic forms. Chirurgie 1997;121:663–666.
9. Cornell CN, Tyndall D, Waller S, Lane JM, Brause BD. Treatment of experimental osteomyelitis with antibiotic-impregnated bone graft substitute. J Orthop Res 1993;11: 619–626.
10. Shinto Y, Uchida A, Koskusuz F, Araki N, Ono K. Calcium hydroxyapatite ceramic used as a delivery system for antibiotics. J Bone Joint Surg Br 1992;74:600–604.
11. Thoma K, Alex R, Randzio J. Biodegradable Gentamycin-depot implants made of β-tricalcium phosphate ceramics. III. *In vivo* studies on drug release, tissue tolerance, and biodegradation. Pharmazie 1991;46:266–270.
12. Buchholz HW, Engelbrecht H. Depot effects of various antibiotics mixed with Palacos resins. Chirurg 1970;41:511–515.
13. Mitsuhashi Y, Susumu K. Drug action and drug resistance in bacteria. Tokyo: University of Tokyo Press; 1975.
14. Penner MJ, Duncan CP, Masri BA. The *in vitro* elution characteristics of antibiotic-loaded CMW and Palacos-R bone cements. J Arthroplasty, 1999;14:209–214.
15. Greene N, Holtom PD, Warren CA, Ressler RL, Sheperd L, McPherson EJ, Patzakis MJ. *In vitro* elution of tobramycin and

vancomycin polymethylmethacrylate beads and spacers from Simplex and Palacos. Am J Orthop 1998;27:201–205.
16. Klekamp J, Dawson JM, Haas DW, DeBoer D, Christie M. The use of vancomycin and tobramycin in acrylic bone cement: Biomechanical effects and elution kinetics for use in joint arthroplasty. J Arthroplasty 1999;14:339–346.
17. Information for Health Professionals Data Sheet. – Tobramycin sulfate. Available: http://www.medsafe.govt.nz/Profs/datasheet/n/nebcininj.html. Accessed 2000.
18. Clinical Pharmacology Online. Tobramycin. Available: http://www.rxlist.com
19. Tobramycin Material Safety and Data Sheet. Available: http://www.hazard.com/msds/index.php
20. Stemberger A, Grimm H, Bader F. Local treatment of bone and soft tissue infections with the collagen-gentamycin sponge. Eur J Surg 1997;578(Suppl):17–26.
21. Rutten HJT, Nijuis PHA. Prevention of wound infection in elective colorectal surgery by local application of a Gentamycin-cotaining collagen sponge. Eur J Surg 1997;578(Suppl):31–35.
22. Otsuka M, Sawada M, Matsuda Y, Nakamura T, Kokubo T. Antibiotic delivery system using bioactive cement consisting of *Bis*-GMA/TEGDMA resin and bioactive glass ceramics. Biomaterials 1997;18:1559–1564.
23. Kawanabe K, Okada Y, Matsusue Y. Treatment of osteomyelitis with antibiotic-soaked porous glass ceramic. J Bone Joint Surg Br 1998;80:527–530.
24. Netz DJA, Sepulveda P, Pandofelli VC, Spadaro ACC, Alencastre JB, Bentley MLVB, Marchetti JM. Potential use of gel casting hydroxyapatite porous ceramic as an implantable drug delivery system. Int J Pharm 2001;213:177–125.
25. Itokazu M, Ohno T, Tanemori T. Antibiotic-loaded hydroxyapatite blocks in the treatment of experimental osteomyelitis in rats. J Med Microbiol 1997;46:779–783.
26. Queiroz AC, Santos JD, Monteiro FJ, Gibson IR, Knowles JC. Adsorption and release studies of sodium ampicillin from hydroxyapatite and glass-reinforced hydroxyapatite composites. Biomaterial 2001;22:1393–1400.
27. Yaylaoglu MB, Koskusuz F, Hasirei V. In: Haris PI, Chapman D, editors. New biomedical materials. Amsterdam: IOS Press; 1998. p 149–154.
28. Bohner M, Lemaitre J, Merkle HP, Gander B. Control of Gentamycin release from a calcium phosphate cement by admixed poly(acrylic acid). J Pharm Sci 2000;89:1262–1270.
29. Bohner M, Lemaitre J, van Landyut P, Zambelli PY, Merkle HP, Gander B. Gentamycin-loaded hydraulic calcium phosphate bone cement as antibiotic delivery system. J Pharm Sci 1997;86:565–572.
30. Thoma K, Alex R, Fensch-Kleemann E. Biodegradable controlled-release implants based on β-tricalcium phosphate ceramic. Part 1. Preparation and characterization of porous β-tricalcium phosphate pellets. Eur J Pharm Biopharm 1992;38:101–106.
31. Thoma K, Alex R, Randzio J. Biodegradable controlled-release implants based on β-tricalcium phosphate ceramic. Part 2. Testing of Gentamycin controlled-release pellets *in-vitro* and *in-vivo*. Eur J Pharm Biopharm 1992;38:107–112.
32. Garvin KL, Miyano JA, Robinson D. Polylactide/polyglycolide antibiotics implants in the treatment of osteomyelitis. J Bone Joint Surg 1994;76A:1500–1506.
33. Tsourvakas S, Hatzigrigorig P, Tsibinos A. Pharmacokinetic study of fibrin clot-ciprofloxacin complex: An *in vitro* and *in vivo* experimental investigation. Arch Orthop Trauma Surg 1995;144:295–297.
34. Schreirholz JM, Steinhauser H, Rump AFE. Controlled release of antibiotics from biomedical polyurethanes: Morphological and structural features. Biomaterials 1997;18:839–844.
35. Vaccaro RA. The role of the osteoconductive scaffold in synthetic bone graft. Orthopedics 2002;25:S572–S578.
36. Kortesuo P, Ahola M, Kangas M, Leino T, Laasko S, Vuorilehto L, Yli-Urpo A, Kiesvaara J, Marvola M. Alkyl-substituted silica gel as a carrier in the controlled release of dexmedetomidine, J Control Rel 2001;76:227–238.
37. Kortesuo P, Ahola M, Karlsson S, Kangasniemi I, Kiesvaara J, Yli-Urpo A. Sol-gel–processed sintered xerogel as a carrier in controlled drug delivery. J Biomed Mater Res 1999;44:162–167.
38. Kortesuo P, Ahola M, Kangas M, Yli-Urpo A, Kiesvaara J, Marvola M. *In vitro* release of dexmedetomidine from silica xerogel monoliths: Effect of sol-gel synthesis parameters. Int J Pharm 2001;221:107–114.
39. Kortesuo P, Ahola M, Kangas M, Kangasniemi I, Yli-Urpo A, Kiesvaara J. *In vitro* evaluation of sol-gel processed spray dried silica gel microspheres as carrier in controlled drug delivery. Int J Pharm 2000;200:223–229.
40. Radin S, Ducheyne P, Kamplain T, Tan BH. Silica sol-gel for the controlled release of antibiotics. I. Synthesis, characterization, and *in vitro* release. J Biomed Mater Res 2001;57:313–320.
41. Aughenbaugh W, Radin S, Ducheyne P. Silica sol-gel for the controlled release of antibiotics. II. The effect of synthesis parameters on the *in vitro* release kinetics of vancomycin. J Biomed Mater Res 2001;57:321–326.
42. Ahola MS, Sailynoja ES, Raitavuo MH, Vaahtio MM, Salonen JI, Yli-Urpo AUO. *In vitro* release of heparin from silica xerogels. Biomaterials 2001;22:2163–2170.
43. Kanellakopoulou K, Glamerellos-Bourbolis EJ. Carrier systems for the local delivery of antibiotics in bone infections. Drugs 2000;59:1223–1232.
44. Atkins B, Gottleib T. Fusidic acid in and joint infections. Int J Antimicrob Agents 1999;12(2 Suppl):S79–S93.
45. Suwanprateeb J, Tanner K, Turner W. Influence of sterilization by gamma irradiation of thermal annealing on creep of hydroxyapatite-reinforced polyethylene composites. J Biomed Mater Res 1998;39:16–22.
46. Assink RA, Kay BD. Sol-gel kinetics by NMR. Polymer Prepr Am Chem Soc Div Polym Chem 1991;32:506–507.
47. Szpalski M, Gunzburg R. Applications of calcium phosphate-based cancellous bone void fillers in trauma surgery. Orthopedics 2002;25(5 Suppl):S601–S609.
48. Bohner M. Calcium orthophosphates in medicine: From ceramic to calcium phosphates cements. Injury 2000;31(4 Suppl):SD37–SD47.
49. Available: http://www.orthovita.com/products/vitoss/index.html
50. Karmakar B, Ganguli D. Sol-gel synthesis and surface activity of alkoxy-derived TiO_2-SiO_2 powders. Indian J Technol 1987;25:282–289.
51. Wei Y, Yang D, Tang L. Synthesis, characterization, and properties of new polystyrene-SiO_2 hybrid sol-gel materials. J Mater Res 1993;8;1143–1152.
52. Wei Y, Xu J, Dong H, Dong JH, Qiu K, Jansen-Varnum SA. Preparation and physisorption characterization of $_D$-glucose-templated mesoporous silica sol-gel materials. Chem Mater 1999;11:2023–2029.
53. Wei Y, Bakthavatchalam R, Yang D, Whitecar CK. Synthesis and characterization of polyacrylate–inorganic hybrid materials via the sol-gel approach. Polym Prepr Am Chem Soc Div Polym Chem 1991;32:503–505.
54. Marsical R, Lopez-Granados M, Fierro JLG, Sotelo JL, Martos C., Van Greiken R. Morphological and surface properties of titania–silica hydrophobic xerogels Langmuir 2000;16:9460–9467.
55. Perdroso MAS, Dias ML, Azuma C, Mothe CG. Hydrocarbon dispersion of nanospherical silica by a sol-gel process. 1. Tetraethoxysilane homopolymerization. Colloid Polym Sci 2000;278:1180–1186.

56. Roy R, Roy DM. Synthesis and stability of minerals in the system $MgO\text{-}Al_2O_3$ $SiO_2\text{-}H_2O$. Am Mineral 1955;40:147–178.
57. Chan CK, Peng SL, Chu IM, Ni SC. Effects of heat treatment on the properties of poly(methyl methacrylate)/silica hybrid materials prepared by sol-gel process. Polymer 2001;42:4189–4196.
58. You WW, Haugland RP, Ryan DK, Haugland RP. 2-(4-Carboxybenzoyl)quinoline-2-carboxyaldehyde, a reagent with broad dynamic range for the assay of proteins and lipoproteins in solution Analyt Biochem 1997;244:277–282.
59. Molecular probes product fact sheet, CBQCA. Available: http://www.molecularprobes.com
60. Zhang Y, Arriaga E, Diedrich P, Hindsgaul O, Dovichi NJ. Nanomolar determination of aminated sugars by capillary electrophoresis. J Chromatogr A 1995;716:221–229.
61. El-Shabrawy Y. Fluorometric determination of aminoglycoside antibiotics in pharmaceutical preparations and biological fluids. Spectrosc Lett 2002;35:99–109.
62. Ragel CV, Vallet-Regi M. *In vitro* bioactivity and Gentamycin release from glass-polymer-antibiotic composites. J Biomed Mater Res 2000;51:424–429.
63. Higuchi T. Mechanism of sustained-action medication. Theoretical analysis of rate of release of solid drugs dispersed in solid matrices. J Pharm Sci 1963;52:1145–1149.
64. Laidler KJ, editor. Chemical kinetics. New York: Harper Collins; 1987.
65. Baker AS, Greenham LW. Release of Gentamycin from acrylic bone cement. J Bone Joint Surg Am 1988;70:1551–1557.
66. Kuechle DK, Landon GC, Musher DM, Noble PC. Elution of vancomycin, daptomycin, and amikacin from acrylic bone cement. Clin Orthop 1991;264:302–308.
67. Hope PG, Kristinsson KG, Norman P, Elson RA. Deep infection of cemented total hip arthroplasties caused by coagulase negative staphylococci. J Bone Surg B 198971: 851–855.
68. DiCicco M, Duong T, Chu A, Jansen SA. Tobramycin and Gentamycin elution analysis between two *in-situ* polymerizable orthopaedic composites. J Biomed Mater Res Appl Biomater. Forthcoming.
69. Chohfi M, Langlais F, Fourastier J, Minet J, Thomazean H, Cormier M. Pharmacokinetics, uses, and limitations of vancomycin-loaded bone cement. Int Orthop 1998;22:171–177.
70. Frutos Cabanillas P, Diez Pena E, Barrales-Rienda JM, Frutos G. Validation and *in vitro* characterization of antibiotic-loaded bone cement release. Int J Pharm 2000209:15–26.
71. Weisman DL, Olmstead ML, Kowalski JJ. *In vitro* evaluation and antibiotic elution from polymethylmethacrylate (PMMA) and mechanical assessment of antibiotic-PMMA composites. Vet Surg 2000;29:245–251.
72. Clineff TD. Bioactivity report: Determination of VITOSS bioactivity by assessing the formation of a superficial hydroxyapatite layer by FTIR. Unpublished internal report. Orthovita, Inc.
73. Greenspan DC. Developments in biocompatible glass compositions. Available: http://www.devicelink.com/mddi/archive/99/03/011.html
74. Ruys AJ. Silicon-doped hydroxyapatite. J Aust Ceram Soc 1993;29: 71–80.